[6] C. Gatti, R. Bianchi, R. Destro, F. Merati, *THEOCHEM* **1992**, *255*, 409.
[7] T. Koritsánszky, J. Buschmann, P. Luger, *J. Phys. Chem.* **1996**, *100*, 10547.
[8] C. Gatti, V. R. Saunders, C. Roetti, *J. Chem. Phys.* **1994**, *101*, 10686.
[9] R. Flaig, T. Koritsánszky, J. Janczak, H.-G. Krane, W. Morgenroth, P. Luger, *Angew. Chem.* **1999**, *111*, 1494; *Angew. Chem. Int. Ed.* **1999**, *38*, 1397.
[10] T. Koritsánszky, R. Flaig, D. Zobel, H.-G. Krane, W. Morgenroth, P. Luger, *Science* **1998**, *279*, 356.
[11] B. B. Iversen, F. K. Larsen, A. A. Pinkerton, A. Martin, A. Darovsky, P. A. Reynolds, *Acta Crystallogr. Sect. B* **1999**, *55*, 363.
[12] S. Dahaoui, C. Jelsch, J. A. K. Howard, C. Lecomte, *Acta Crystallogr. Sect. B* **1999**, *55*, 226.
[13] P. Coppens, *X-Ray Charge Densities and Chemical Bonding*, Oxford University Press, Oxford, **1997**.
[14] R. Soyka, B. D. Guth, H. M. Weisenberger, P. Luger, T. H. Müller, *J. Med. Chem.* **1999**, *42*, 1235.
[15] J. Wouters, F. Durant, B. Masereel, *Bioorg. Med. Chem. Lett.* **1999**, *9*, 2867.
[16] Crystallographic data: $C_{23}O_2N_5H_{27}$, $M_r = 405.49$, monoclinic $P2_1/a$, $a = 14.832(2)$, $b = 10.097(1)$, $c = 15.599(2)$ Å, $\beta = 113.55(1)^\circ$, $V = 2141.52$ Å^3, $Z = 4$, $\rho_{calcd} = 1.258$ g cm^{-3}, $Mo_{K\alpha}$ radiation ($\lambda = 0.7107$ Å), $T = 100$ K, Bruker-AXS SMART diffractometer, CCD area detector, 219870 measured reflections, 39356 unique, $d = 0.4$ Å, $\sin\theta/\lambda_{max} = 1.25$ Å^{-1}, $R(F) = 0.0236$, $R_w(F) = 0.0180$ after multipole refinement, hexadecapolar for C, N, O, one quadrupole, otherwise dipoles for H. Crystallographic data (excluding structure factors) for the structures reported in this paper have been deposited with the Cambridge Crystallographic Data Centre as supplementary publication no. CCDC-147443. Copies of the data can be obtained free of charge on application to CCDC, 12 Union Road, Cambridge CB2 1EZ, UK (fax: (+44) 1223-336-033; e-mail: deposit@ccdc.cam.ac.uk).
[17] Gaussian 94, Revision E.2, Gaussian, Inc., Pittsburgh, PA, **1995**.
[18] T. Koritsánszky, S. Howard, T. Richter, Z. W. Su, P. R. Mallinson, N. K. Hansen, *XD—A Computer Program Package for Multipole Refinement and Analysis of Electron Densities from Diffraction Data. User Manual*, Freie Universität Berlin, **1995**.
[19] The ellipticity ε is defined by $(\lambda_1/\lambda_2) - 1$, with λ_1 and λ_2 being the two principal curvatures of $\rho(\boldsymbol{r})$ at a BCP, and is a measure of the aspherical nature of the charge in a chemical bond.
[20] Z. Su, P. Coppens, *Acta Crystallogr. Sect. A* **1992**, *48*, 188.
[21] J. Gao, C. Alhambra, *J. Am. Chem. Soc.* **1997**, *119*, 2962.
[22] M. A. Spackman, *Chem. Rev.* **1992**, *92*, 1769.
[23] M. N. Burnett, C. K. Johnson, *ORTEP-III*, *Oak Ridge Thermal Ellipsoid Plot Program for Crystal Structure Illustrations*, Oak Ridge National Laboratory, **1996**.

Polyol-Mediated Preparation of Nanoscale Oxide Particles**

Claus Feldmann* and Hans-Otto Jungk

Nanoscale oxide particles with a mean particle diameter of 30 to 300 nm are gaining increasing technical importance for classic areas of application such as catalysts, passive electronic components, or ceramic materials.[1] However, they also contribute in an essential way to the realization of completely new concepts such as transparent solar cells[2] or photonic crystals.[3] In addition, they play an important role in the selective surface modification (e.g. passivation, hardening, coloration) of various substrates in the form of coatings.[4] With regard to all of the applications mentioned, in addition to the particle size a low degree of agglomeration and a monodisperse size distribution are desirable to enable a homogeneous arrangement of particles in thin films or as coatings. The polyol method applied herein provides a promising preparative approach to such oxide particles.

The polyol method was initially described for the preparation of elemental metals and alloys,[5] in which the reducing properties of a high-boiling alcohol (e.g. glycerol, glycol) towards a suitable metal precursor were utilized. With regard to oxidic materials, only a few insights have been gained so far, namely for ZnO, Fe_2O_3, $CoAl_2O_4$, and Bi_2O_3.[6] Our investigations show that the polyol method, which can also be understood as a sol–gel process carried out at elevated temperatures in the case of oxides, is suitable for the preparation of a host of binary and ternary oxides.

By heating suitable metal salts and a defined amount of water in diethylene glycol (DEG), suspensions of various materials are obtained in a simple manner (Figure 1, Table 1). These oxide particle suspensions are colloidally stable and can contain up to 20 wt % of solids. A detailed characterization of the oxide particles obtained is exemplified for Cu_2O, TiO_2,

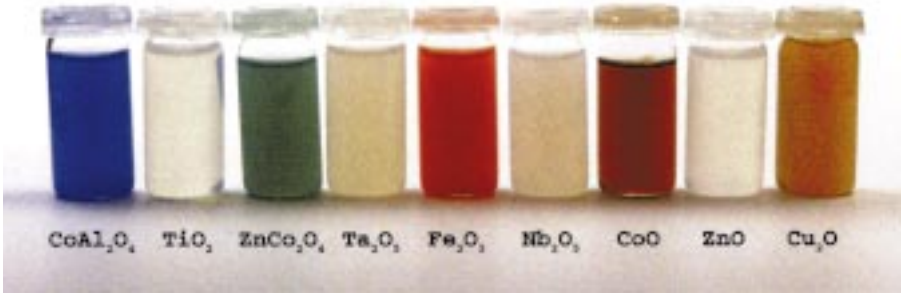

Figure 1. Various oxide particle suspensions in DEG.

[*] Dr. C. Feldmann, H.-O. Jungk
Philips GmbH
Forschungslaboratorien
52066 Aachen (Germany)
Fax: (+49) 241-6003-465
E-mail: claus.feldmann@philips.com

[**] We thank Jacqueline Merikhi and Gerd Much for carrying out the scanning electron microscopy (SEM) and the atomic force microscopy (AFM) investigations, respectively.

  1433-7851/01/4002-0359 $ 17.50+.50/0

Table 1. Nanoscale oxide particles obtained with the polyol method.

Cu_2O	CoO	Al_2O_3	SiO_2	V_2O_5	MoO_3	$MgAl_2O_4$
	ZnO	Bi_2O_3	SnO_2	Nb_2O_5	WO_3	$BaAl_2O_4$
	CdO	Y_2O_3	TiO_2	Ta_2O_5		$CoAl_2O_4$
		La_2O_3	ZrO_2			$ZnCo_2O_4$
		Cr_2O_3				
		Fe_2O_3				

and Nb_2O_5. Monodisperse and nanoscale TiO_2 particles can also be obtained by other preparative methods;[7] Cu_2O and Nb_2O_5, on the other hand, have so far only been described as unstructured or amorphous films, respectively, or as particles with a very inhomogeneous size distribution. Moreover, the preparation was carried out at comparatively high temperatures (500–1000 °C) in both cases.[8, 9]

The oxide particles prepared with the polyol method can be investigated more closely after separation from the suspension by centrifugation. The resulting powders are highly crystalline (Figure 2) immediately after their synthesis at a maximum temperature of 180 °C (e.g. Cu_2O, TiO_2) or after short heating to surprisingly low temperatures (e.g. Nb_2O_5, 15 min at 300 °C). Electron micrographs show spherical, nanoscale and largely monodisperse oxide particles (Figure 3). By modifying the experimental conditions, especially the concentrations of the metal precursor and of water, a mean particle diameter between about 30 and 200 nm can be realized.[6] The spherical habit of the oxide particles is attributed predominantly due to the coverage of the growth areas with the chelating agent diethylene glycol. This suppresses an inhomogeneous growth of the nuclei. Differential thermal analysis (DTA)/thermogravimetric (TG) studies prove that the DEG film adhering to the particle surfaces can be removed completely by heating to 250 °C. The powdered materials then show Brunauer–Emmett–Teller (BET) surfaces of around 100 $m^2 g^{-1}$.

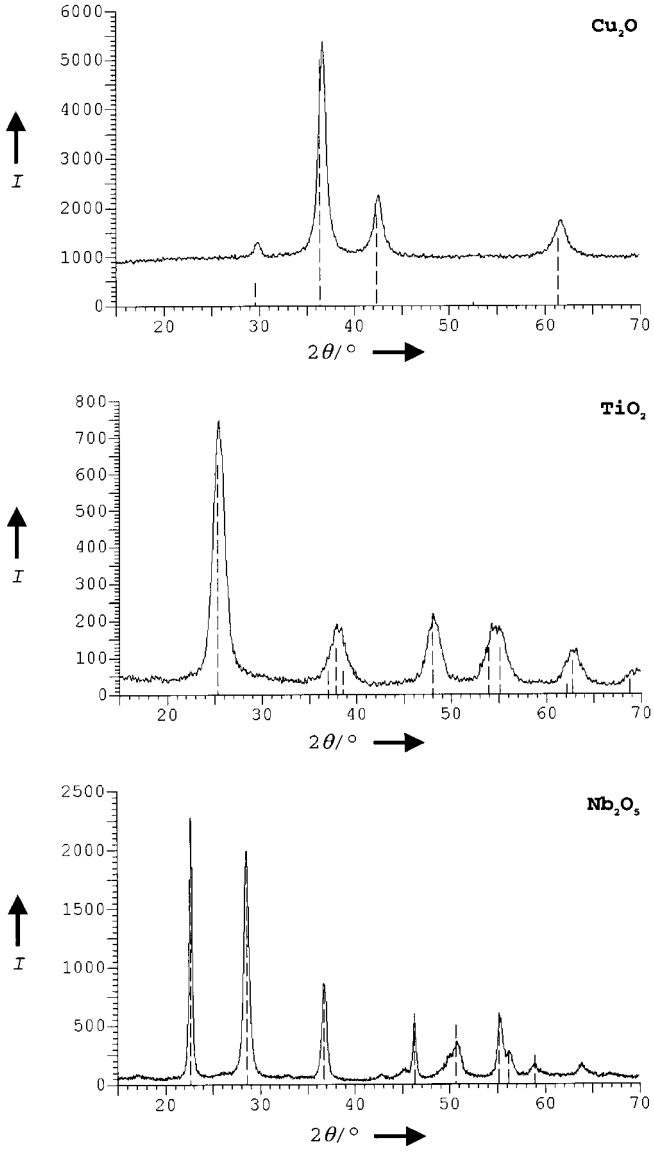

Figure 2. Powder diffractograms of Cu_2O (ICDD-Ref. 05-0667/cuprite), TiO_2 (ICDD-Ref. 21-1272/anatase), and Nb_2O_5 (ICDD-Ref. 28-0317).

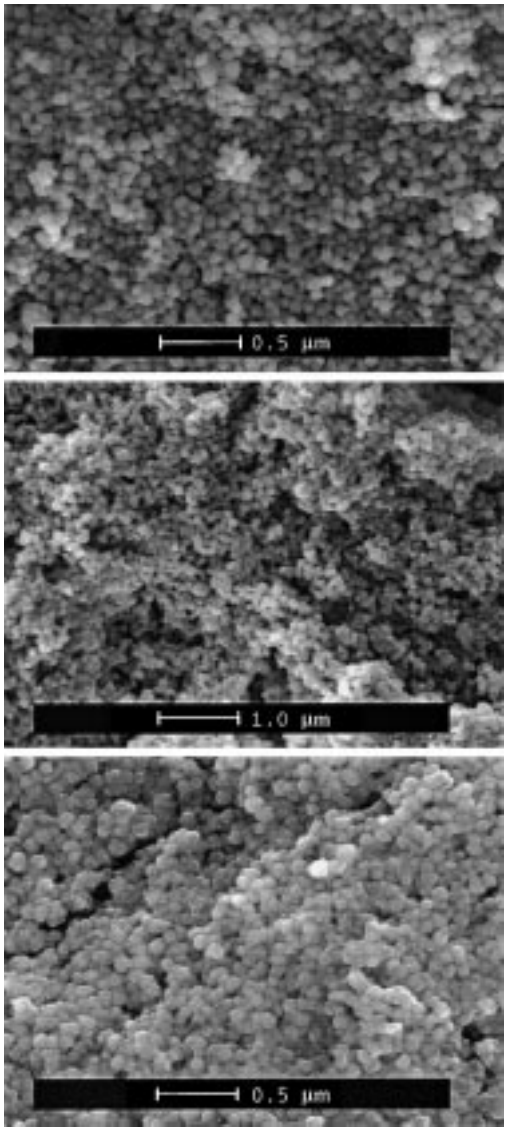

Figure 3. Electron micrographs of Cu_2O (top), TiO_2 (middle), and Nb_2O_5 particles (bottom).

Laser diffraction investigations of oxide particle suspensions confirm the mean particle diameters determined by

  1433-7851/01/4002-0360 $ 17.50+.50/0

scanning electron microscopy (SEM) of powders (Figure 4). Thus, individual, non-agglomerated oxide particles are present in the suspension. This is all the more remarkable as no

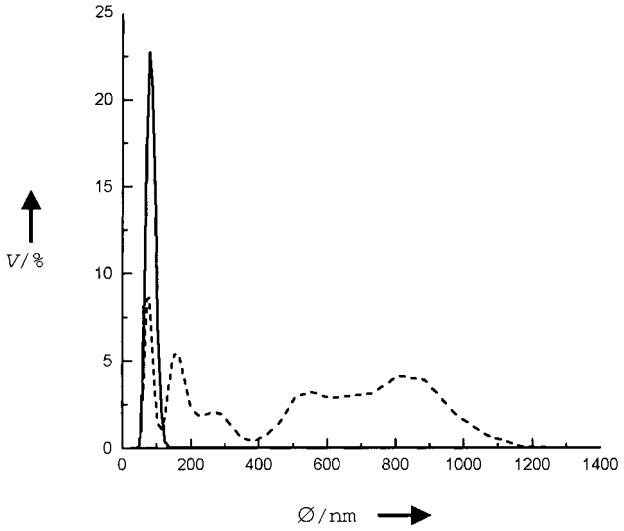

Figure 4. Particle diameters (∅) of Nb_2O_5 particles in DEG (——) and 30 min after mixing with water (- - - -).

further stabilizing agents apart from DEG are required. If, however, the DEG suspension is mixed with water, the colloid breaks down and rapid agglomeration of the oxide particles occurs (Figure 4). In the presence of a suitable substrate, the destabilization of the colloid can be used for the selective adhesion of oxide particles to the surface of the substrate. With common methods such as dipping or spin-coating, thin and homogeneous oxide particle layers can be applied to planar substrates, for example a glass plate (Figure 5). In addition, substrates with a curved surface can be coated homogeneously. Thus, the substrate itself, for example Al_2O_3 powder, can consist of particles (Figure 5). Taking the relevant parameters (e.g. polarity and charge of the surface) into consideration,[10] a virtually immediate and reliable adhesion between substrate and oxide particles is obtained. The coverage of the Al_2O_3 surface with individual, nanoscale Nb_2O_5 particles achieved in the example shown here can be considered as further support for the presence of non-agglomerated oxide particles in the DEG suspension.

The broad applicability and the opportunity to produce nanoscale and crystalline oxides at moderate temperatures are the key features of the polyol method. The comparatively high solid content coupled at the same time with the absence of additional stabilizers makes the oxide particle suspensions in diethylene glycol of technical interest for the coating and modification of surfaces. Preliminary investigations have now also shown that, besides oxides, sulfides (e.g. ZnS) and phosphates (e.g. $LaPO_4$) can be produced in the form of nanoscale particles with the polyol method.[11]

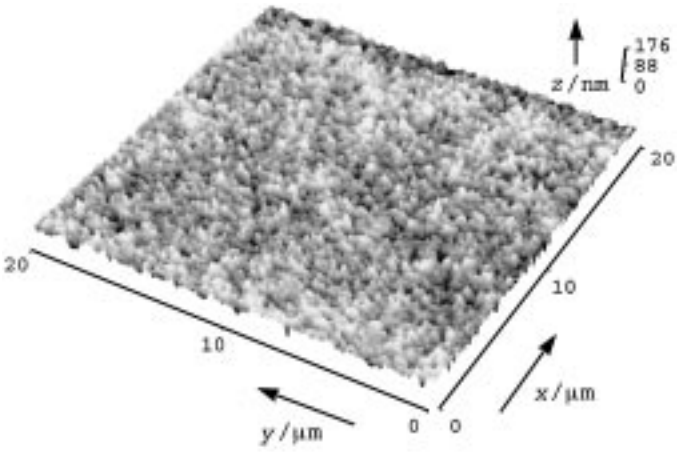

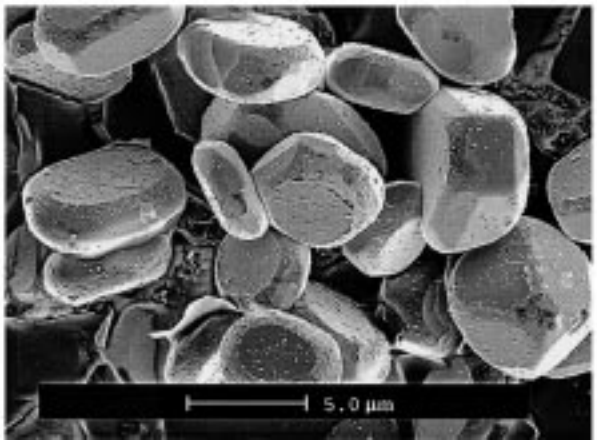

Figure 5. Coverage of a glass plate (top) and an Al_2O_3 powder (bottom) with Nb_2O_5 particles.

Experimental Section

To prepare Cu_2O, TiO_2, and Nb_2O_5 oxide particles, DEG (50 mL; 99.9 %; Merck) was placed in a 250 mL round-bottomed flask. A solution of $Cu(CH_3COCHCOCH_3)_2$ (2.3 mM; 99 %; Alfa), $Ti(OiPr)_4$ (2.3 mM; 99.999 %; Aldrich), or $Nb(OC_2H_5)_5$ (2.3 mM; 99.95 %; Heraeus) was added, under vigorous stirring, and the clear solution was heated to 140 °C. Subsequently, demineralized water (2 mL) was added and the mixture was heated to 180 °C for 2 h. After the mixture had been cooled, the solid was separated by centrifuging the suspension. It was then resuspended twice in ethanol and centrifuged again to remove any remaining DEG. For the coverage of planar substrates (e.g. glass plates), the oxide particle suspensions in DEG were mixed with water in ratios of 1:1 to 1:10. These mixtures were applied to the substrates by dipping or spin-coating. Powdered substrates (e.g. Al_2O_3 particles) were suspended in water, and the DEG suspension was slowly added dropwise.

The powder diffraction spectra were recorded with a Philips goniometer PW1050 with Bragg-Brentano geometry (graphite monochromator, proportional counter, $Cu_{K\alpha}$ radiation). The electron micrographs were obtained with a Philips/FEI-scanning electron microscope XL30 (samples treated with carbon vapor, accelerating potentials 5–10 kV). The particle sizes in suspension were determined with a Coulter LS230 instrument (Laser power 5 mW at 750 nm, halogen lamp with 150 lm at 2900 K, detector with 126 photodiodes). A Topometrix Explorer was used for the atomic force microscopy (AFM) experiments (Si_3N_4 tip, vertical distance <2 µm, lateral distance <150 µm).

Received: August 10, 2000 [Z15617]

[1] a) H. Gleiter, *Prog. Mater. Sci.* **1989**, *33*, 223; b) D. Hennings, M. Klee, R. Waser, *Adv. Mater.* **1991**, *3*, 334; c) J. H. Fendler, *Nanoparticles and Nanostructured Films*, 1st ed., Wiley-VCH, Weinheim, **1998**; d) L. V. Interrante, M. J. Hampten-Smith, *Chemistry of Advanced Materials*, 1st ed., Wiley-VCH, Weinheim, **1998**; e) K. Hoshino, M. Inui, T.

  1433-7851/01/4002-0361 $ 17.50+.50/0

Kitamura, H. Kokado, *Angew. Chem.* **2000**, *112*, 2558, *Angew. Chem. Int. Ed.* **2000**, *39*, 2509.
[2] a) B. O'Regan, M. Grätzel, *Nature* **1991**, *353*, 737; b) A. Hagfeldt, M. Grätzel, *Chem. Rev.* **1995**, *95*, 49.
[3] a) G. Subramanian, V. N. Manoharan, J. D. Thorne, D. J. Pine, *Adv. Mater*. **1999**, *11*, 1261; b) O. D. Velvev, E. W. Kaler, *Adv. Mater*. **2000**, *12*, 531; c) Y. Xia, B. Gates, Y. Yin, Y. Lu, *Adv. Mater*. **2000**, *12*, 693.
[4] a) H. K. Pulker, *Coatings on Glass*, Elsevier, Amsterdam, **1984**; b) R. J. Hunter, *Introduction to Modern Colloid Science*, Oxford Science Publications, Oxford, **1992**; c) J. B. Wachtman, R. A. Haber, *Ceramic Films and Coatings*, Noyes Publications, Park Ridge, **1993**.
[5] a) F. Fievet, J. P. Lagier, M. Figlarz, *Mater. Res. Bull.* **1989**, 29; b) L. K. Kurihara, G. M. Chow, P. E. Schoen, *Nanostruct. Mater.* **1995**, *5*, 607; c) P. Toneguzzo, G. Viau, O. Acher, F. Fievet-Vincent, F. Fievet, *Adv. Mater*. **1998**, *10*, 1032; d) S. Sun, C. B. Murray, D. Weller, L. Folks, A. Moser, *Science* **2000**, *287*, 1989.
[6] a) D. Jezequel, J. Guenot, N. Jouini, F. Fievet, *J. Mater. Res.* **1994**, *10*, 77; b) J. Merikhi, H.-O. Jungk, C. Feldmann, *J. Mater. Chem.* **2000**, *10*, 1311; c) H.-O. Jungk, C. Feldmann, *J. Mater. Res.* **2000**, *15*, 2244; d) J. Merikhi, C. Feldmann, *J. Mater. Sci.*, in press.
[7] a) E. Matijevic, *Langmuir* **1986**, *2*, 12; b) J. Livage, M. Henry, C. Sanchez, *Prog. Solid State Chem.* **1988**, *18*, 259; c) E. Matijevic, *Chem. Mater*. **1993**, *5*, 412; d) M. Ocana, R. Rodriguez-Clemente, C. J. Serna, *Adv. Mater*. **1995**, *7*, 212; e) H. Herrig, R. Hempelmann, *Mater. Lett.* **1996**, *27*, 287; f) G. L. Li, G. H. Wang, *Nanostruct. Mater*. **1999**, *11*, 663; g) Y. Juan, M. Sen, M. F. Ferreira, *J. Am. Ceram. Soc.* **2000**, *83*, 1417.
[8] a) T. Takahashi, J. Suzuki, M. Saburi, Y. Uchida, *J. Mater. Sci. Lett.* **1988**, *7*, 1251; b) D. Majumdar, T. A. Shefelbine, T. T. Kodas, H. D. Glicksman, *J. Mater. Res.* **1996**, *11*, 2861.
[9] a) M. Guenin, R. Frey, E. Garbowski, P. Vergnon, *J. Mater. Sci*. **1988**, *23*, 1009; b) N. P. Bansal, *J. Mater. Sci.* **1994**, *29*, 4481; c) N. Özer, D. G. Chen, C. M. Lampert, *Thin Solid Films* **1996**, *277*, 162.
[10] a) N. Kallay, *Mater. Res. Bull*. **1990**, 41; b) D. Myers, *Surfaces, Interfaces and Colloids*, 2nd ed., Wiley-VCH, Weinheim, **1999**; c) J. Merikhi, C. Feldmann, *J. Colloid Interface Sci*. **2000**, *223*, 229.
[11] H.-O. Jungk, C. Feldmann, *J. Mater. Chem.*, submitted.

Counter-Rotating Ring Currents in Coronene and Corannulene**

Erich Steiner, Patrick W. Fowler, and Leonardus W. Jenneskens*

Ring currents are intimately linked with the concept of aromaticity in organic chemistry and are essential ingredients of the interpretation of physical and chemical properties of conjugated π systems.[1–7] The currents themselves are not directly observable, but are inferred through their manifestations in NMR spectroscopy and measurements of magnetic anisotropy ("exaltation of diamagnetism").[8] In monocyclic systems, diamagnetic circulations are associated with the magic Hückel count of $4n+2$ π electrons. In fused polycyclic systems such as the planar coronene (**1**) and the bowl-shaped corannulene (**2**; Scheme 1), it is traditional to invoke an

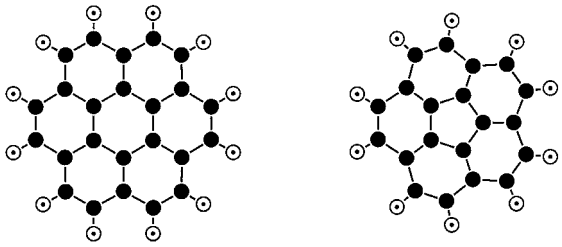

1 **2**

Scheme 1. ● = carbon; ⊙ = hydrogen.

"annulene-within-an-annulene" model,[9, 10] in which both rim and hub attain the aromatic Hückel count (18 and 6 in **1**, and 14 and 6 in **2** if the transfer of one electron to the central pentagon is invoked), which implies there are conrotatory diamagnetic ring currents in the two cycles. Against this picture, calculated populations[11] show no significant redistribution of electron density from rim to hub in **2**, and the "nucleus-independent chemical shift" (NICS), proposed as a criterion of aromaticity by Schleyer et al.,[12] indicates that both **1** and **2** have outer aromatic (diamagnetic, diatropic) but inner non-aromatic or anti-aromatic (paramagnetic, paratropic) circuits.[13]

Fortunately, distributed-origin methods developed in recent years[14–19] allow the accurate calculation of magnetic response properties and, in particular, direct visualization of induced current densities in conjugated systems.[20–22] They are used here to confront the discrepant models of **1** and **2** with an ab initio computation of the ring currents, and, additionally, to discuss the question of the applicability of π-only pictures to the nonplanar, bowl-shaped corannulene systems, and hence to fullerenes.[23, 24] Thus, computational comparisons are made between coronene (**1**, D_{6h}) and corannulene (**2**) in both the equilibrium C_{5v} bowl configuration and the planar D_{5h} transition state for bowl-to-bowl conversion.

Computed current-density maps (see Experimental Section) are shown in Figure 1 for the σ, π, and total (σ+π) electrons at $1\,a_0$ above the molecular planes of **1** and planar **2**. The σ maps at this height do not show the detail of the current density close to the nuclei but they do demonstrate characteristic superpositions of diamagnetic circulations centred on σ bonds, with a cumulative effect within each ring of a net central paramagnetic circulation. In both molecules **1** and **2** the π currents combine to give a clear diamagnetic circulation around the outer rim with a paramagnetic counter-circulation on the inner hub. In detail, slight differences can be found between the two molecules: in **1** the outer circulation is stronger than the inner, whereas in **2** it is the inner that is stronger and residual circulation within radial C–C bonds is evident in **2**. This latter effect is not observed in **1**.

[*] Prof. Dr. L. W. Jenneskens
Debye Institute
Department of Physical Organic Chemistry
Utrecht University
Padualaan 8, 3584 CH Utrecht (The Netherlands)
Fax: (+31) 30-253-4533
E-mail: jennesk@chem.uu.nl
Dr. E. Steiner, Prof. Dr. P. W. Fowler
School of Chemistry, University of Exeter
Stocker Road, Exeter EX4 4QD (UK)

[**] We are grateful for a travel grant from the Council for Chemical Sciences of the Netherlands Organization for Scientific Research (CW-NWO) and the British Council.

  1433-7851/01/4002-0362 $ 17.50+.50/0